PROCEEDINGS OF THE INTERNATIONAL CONFERENCE NANOMATERIALS: APPLICATIONS AND PROPERTIES
Vol. **1** No 4, 04FCNF01(5pp) (2012)

New Ultra Small Iron-Oxide Nanoparticles With Titanium-Carbamate Coating: Preparation and Magnetic Properties

S. Dolci[1,2,*], V. Domenici[1], Z. Jaglicic[3], G. Pampaloni[1]

[1] *Dipartimento di Chimica e Chimica Industriale, Via Risorgimento 35, 56126 Pisa, Italy*
[2] *IMAGO7 Research Foundation ONLUS, Viale del Tirreno 331, 56128 Calambrone (Pisa), Italy*
[3] *Institute of Mathematics, Physics and Mechanics & Faculty of Civil and Geodetic Engineering, University of Ljubljana, Jadranska 19, 1000 Ljubljana, Slovenia*

(Received 03 July 2012; published online 18 July 2012)

This work deals with the preparation and chemical characterization of new Ultra-Small Iron-Oxide Superparamagnetic Nanoparticles (USPIONs) functionalized with Titanium-carbamate. The synthesis was performed starting from oleate-coated and 2-pyrrolidone-coated USPIONs having a maghemite (γ-Fe_2O_3) and magnetite (Fe_3O_4) crystalline core, respectively. Zero-field-cooled (ZFC) and field-cooled (FC) magnetic susceptibility curves as well as the magnetization behavior as a function of temperature are reported and discussed in view of the superparamagnetic properties and coating effect of these new magnetic nanoparticles.

Keywords: Iron oxide nanoparticles, Titanium, Surface coating, Superparamagnetism, USPION, Microscopy.

PACS numbers: 81.07.Bc, 33.25. – k, 62.23.St, 75.20. – g

1. INTRODUCTION

The interest in SuperParamagnetic Iron-Oxide Nanoparticles (SPIONs) is related to recent applications in the field of molecular imaging [1, 2], magnetic resonance imaging (MRI) contrast agents [3-5], drug target delivering [6, 7] and in vivo theranostics [8-10]. As put in evidence by these studies [1-10], the possibility to have successful biomedical applications is related to the biocompatibility of the surface coating [11-12] and to their selective functionalization [13-15].

In particular, the effectiveness of these nanoparticles as MRI contrast agents is related to their magnetic properties, namely their superparamagnetism [3-5]. For instance, magnetite and maghemite iron-oxide nanoparticles are known to behave as superparamagnetic systems [16] and, depending on the magnetic core size, they can act as negative MRI contrast agents, namely reducing the transverse relaxation time, T_2 (or T_2*), or positive MRI contrast agents, giving in brighter signals due to the shortening of the longitudinal relaxation time, T_1. In this respect, the average core size dimensions of these nanoparticles play a fundamental role and it is usually accepted to distinguish between iron oxide nanocrystals with magnetic core larger than 5 nm of diameter (SPIONs) and those with magnetic core smaller than 5 nm of diameter, namely Ultrasmall SPIONs (called USPIONs) [2, 6].

Recently many studies appeared in which the magnetic properties were varied and tuned by doping both SPIONs and USPIONs with metals [17, 18] or by appropriate surface functionalization [19-22]. For instance, the presence of metal ions (such as Mn, Co, Au) having diamagnetic, ferromagnetic or paramagnetic intrinsic behaviour to fill iron oxide crystal vacancies is known to have an effect on the overall magnetic behaviour of the iron-oxide nanomaterials [23].

Another important aspect, especially for MRI contrast agent applications, is the possibility to control both the size-distribution of the nanoparticles [17] and the eventual cluster formation [24].

In this work we are reporting the preparation of new highly monodispersed USPIONs, with average core diameter of about 4 nm, having an external shell made of Titanium-carbamate coating. Two kind of systems were explored: the first one has been prepared starting from oleate-coated USPIONs [25] (with maghemite core: γ-Fe_2O_3) (see Fig. 1) and the second one has been prepared from 2-pyrrolidone-coated USPIONs [26] (with magnetite core: Fe_3O_4).

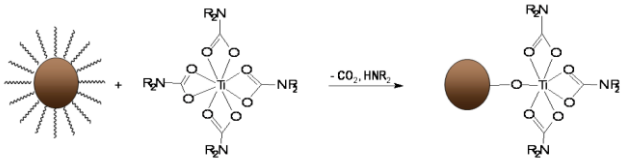

Fig. 1 – Scheme of preparation of the Titanium-carbamate ultrasmall superparamagnetic iron-oxide nanoparticles (Ti-NPs) starting from oleate-coated USPIONs (OA-NPs), by ligand exchange reaction, as described in the text

These new USPIONs have been chemically characterized and a detailed investigation of the magnetic properties, namely zero-field-cooled (ZFC) and field-cooled (FC) magnetic susceptibility curves and the magnetization behavior as a function of temperature, is reported and discussed in view of possible applications.

2. MATERIALS

2.1 Synthesis of oleate coated iron oxide nanoparticles (OA-NP)

$Fe(CO)_5$ (0.66 mL, 5 mmol) was added to a solution of oleic acid (1.59 mL, 5 mmol) in dioctyl ether (50 mL) at 373 K, under nitrogen atmosphere. The

* s.dolci@ns.dcci.unipi.it

mixture was heated to reflux (559 K) and kept at that temperature for 1 h. After cooling to room temperature, anhydrous trimethylamine N-oxide (376 mg, 5 mmol) was added and the mixture was heated to 413 K for 2 h. The reaction was then heated to reflux again for 1 h. The mixture was cooled to room temperature and ethanol was added to obtain the precipitation of nanoparticles, which was then separated by centrifugation and dried with vacuum pump.

2.2 Synthesis of 2-Pyrrolidone coated iron oxide nanoparticles (Py-NP)

$Fe(acac)_3$ (7.10 g, 20 mmol) was added to 2-pyrrolidone (200 mL), that had been previously deoxygenated by vacuum-nitrogen cycles. The mixture was refluxed (518 K) for 30 minutes and, after cooling to room temperature, a solution of methanol: diethyl ether 1:3 was added to obtain the precipitation of nanoparticles. The solid was washed with acetone, collected by centrifugation and dried with vacuum pump.

2.3 Synthesis of Ti(O2CNEt2)4 coated iron oxide nanoparticles (Ti-NP)

$Ti(O_2CNEt_2)_4$, synthesized according to the literature, [27] was dissolved in toluene and OA-NPs or Py-NPs were added. The molar ratio between the coating molecules of nanoparticles (oleate or 2-pyrrolidone) and the carbamate in the mixture was 2:3. The suspension was stirred at reflux temperature (383 K) for 4h. Then, the mixture was concentrated to dryness and the residual brown solid was washed with acetonitrile (2 × 20 mL). Finally, the solid was dried in vacuo and stored in sealed vials under argon atmosphere. In case of Ti-NPs prepared from OA-NPs, two samples with [Ti] equal to 3 % and 0.7 % in weight were investigated.

2.4 Experimental methods

All manipulations of air and/or moisture sensitive compounds were performed under an atmosphere of nitrogen or argon using standard Schlenk techniques. The reaction vessels were oven dried at 150°C prior to use, evacuated (10^{-2} mmHg) and then filled with nitrogen or argon. Solvents were dried according to the conventional methods.

The metal composition of nanoparticles was determined by UV-VIS spectroscopy. The samples were treated with HNO_3 (70 %) and heated to 373 K until complete dissolution, then the iron content was determined by the colorimetric method of ferric thiocyanate (UV absorption band: 480 nm) [28] and titanium content by the hydrogen peroxide method (UV absorption band: 410 nm). [28] The UV-VIS spectra were recorded at 298 K on a UV-VIS Spectrometer PerkinElmer Lambda EZ 201. The IR spectra of the solids were measured at 298 K with a Spectrum One FT-IR Perkin Elmer Spectrometer, equipped with a UATR sampling accessory.

Magnetization (M) and Magnetic Susceptibility (χ) measurements on the NPs powders were conducted on a Quantum Device MPMS-XL-5 Superconducting QUantum Interference Device (SQUID) magnetometer equipped with a 50 kOe magnet. Susceptibility $\chi(T)$ was recorded in a temperature range 5-300 K with a magnetic field H = 100 Oe and isothermal magnetization data $M(H)$ were obtained at 300 K and 5 K in the range – 50 ÷ 50 kOe.

3. RESULTS

In order to obtain highly monodisperse nanoparticles, the USPIONs were prepared by following the thermal decomposition method [25]. Oleate-coated (OA) and 2-pyrrolidone-coated (Py) nanoparticles were prepared as described in the previous section and the resulting OA-NPs and Py-NPs were characterized as reported in the literature [25, 26, 29, 30], thus confirming an average magnetic core diameter of about 4 nm and low polydispersity. A detailed investigation based on microscopy techniques is in progress [31].

Starting from these OA-NPs and Py-NPs, a ligand-exchange reaction was adopted to replace the native monolayer of oleate or 2-pyrrolidone with carbamate ligands, namely the $Ti(O_2CNEt_2)_4$ (see Fig. 1).

FT-IR spectra of the powder samples were acquired and the presence of characteristic signals of carbamate complex and the absence of absorptions of oleate or 2-pyrrolidone confirm that the exchange reaction was successful in all cases.

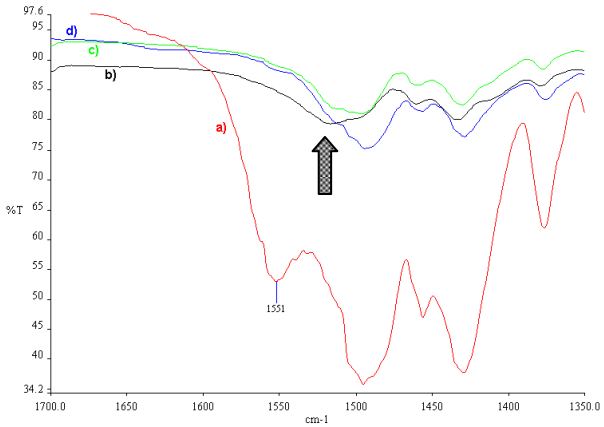

Fig. 1 – Selection of FT-IR spectra of: a) $Ti(O_2CNEt_2)_4$ (red), b) Ti-NPs prepared from OA-NPs with [Ti] = 0.7 % (black) and c) with [Ti] = 3 % (green), d) Ti-NPs prepared from Py-NPs with [Ti] = 2.9 % (blu)

Moreover, the comparison between the spectra of Ti-NPs and the $Ti(O_2CNEt_2)_4$ suggests a coordination of the metal center of complex on the iron oxide surface [32]. Fig. 2 shows the significant difference between the ν_{COO} stretching of the carbamato ligands in $Ti(O_2CNEt_2)_4$ (ν_{COO} = 1551 cm^{-1}) and in the Ti-NPs prepared from both OA-NPs and Py-NPs (ν_{COO} ~ 1516 cm^{-1}) (see the grey arrow).

The magnetization properties of the new Titanium-based USPIONs have been investigated and compared with those of the native NPs: OA-NPs and Py-NPs, respectively. In Figs. 3(a), 3(b) and **4** the magnetization curves of the series of USPIONs derived from the oleate-coated NPs are reported as a function of the applied magnetic field. Here, the values of the magnetization

are normalized with respect to the Fe_2O_3 contained in the core. The amounts of iron were indeed determined by UV-vis spectroscopy, as described in the Experimental section. In particular, the OA-NPs contain 40.3 % in weight of Fe, while the two samples of Ti-NPs having 3 % and 0.7 % of Titanium contain 18.4 % and 19.6 % in weight of Fe, respectively.

Both trends of magnetization recorder at 300 K and 5 K show a typical superparamagnetic behavior and a higher saturation value of the magnetization is observed in case of Titanium-carbamate coated NPs with respect to OA-NPs (see Figs. 3(a) and 3(b) and Table 1).

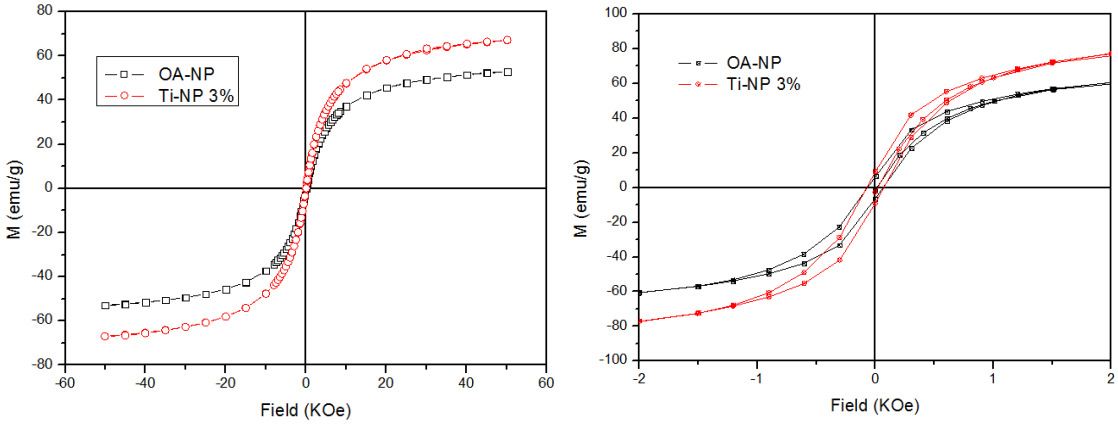

Fig. 3 – (a) Trend of the magnetization M (emu/g of Fe_2O_3) measured at 300 K as a function of the external magnetic field H (kOe) of the OA-NPs (squares) and $Ti(O_2CNEt_2)_4$-NP (circles) with [Ti] = 3 %; (b) Trend of the magnetization M (emu/g of Fe_2O_3) measured at 5 K as a function of the external magnetic field H (kOe) of the OA-NPs (squares) and $Ti(O_2CNEt_2)_4$-NP (circles) with [Ti] = 3 %

From the saturation values of the magnetization recorded at 300 K the average diameters of the nanoparticles was calculated. In fact, if we assume to have a monodispersed sample, the M(H)-dependence can be approximately described by the Langevin theory of paramagnetism [33]:

$$M(H) = M_S L\left[m_p H / (k_B T)\right] \qquad (3.1)$$

where M_S is the saturation magnetization, L is the Langevin function and m_p is the particle's magnetic moment. The saturation values of the magnetization for this series of nanoparticles derived from OA-NPs are reported in Table 1.

If we assume the NPs to have spherical shape, the mean particle diameter d can be estimated using the following equation:

$$m_p = M_0 V = M_S \pi d^3 / 6 \qquad (3.2)$$

where M_0 is the bulk value of magnetization for magnetite nanoparticles. The full lines in Figs. 3 and 4 represent the best fits of the experimental magnetization curves according with Eq. (1).

In all cases the fits confirm an average diameter core of about 4 nm, however a detailed investigation of the morphology of these nanoparticles is in progress [32]. As reported in Figures 5 and 6, the zero-field cooled and field cooled (ZFC/FC) curves represent the typical behaviour of a set of single domain NPs and the average blocking temperature for the OA-NP and Ti-NP samples is reported in Table 1. Moreover, as seen from Fig. 6, the samples containing Titanium-carbamate have a similar magnetic behavior.

Similarly to the oleate-coated nanoparticles, the magnetic properties of the series of USPIONs prepared from the 2-pyrrolidone NPs have been investigated. In this case, the magnetization values have been scaled in respect with the Fe_3O_4 content, since the magnetic crystalline core is made of magnetite [26]. The [Fe], as determined by UV-vis absorption, was found 41.7 % and 30.4 % w/w for Py-NPs and Ti-NPs prepared from them, respectively.

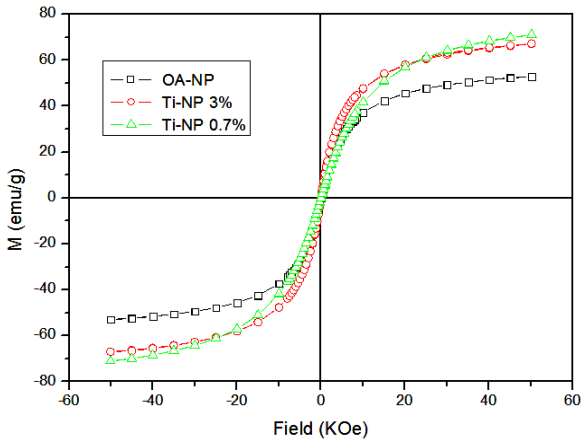

Fig. 4 – Trend of the magnetization M (emu/g of Fe_2O_3) measured at 300 K as a function of the external magnetic field H (kOe) of the OA-NPs (squares), $Ti(O_2CNEt_2)_4$-NP with 3 % (w/w) of Ti (circles), $Ti(O_2CNEt_2)_4$-NP with 0.7 % (w/w) of Ti (triangles)

Table 1 – Saturation magnetization Ms (emu/g of Fe_2O_3) of NPs at 300 K and 5 K and blocking Temperature T_B(K) for the series of NPs derived from OA-NPs.

Samples	*Ms* (T = 300 K)	*Ms*(5 K)	T_B
OA-NP	52	71	12.2
Ti-NP 3%	67	93	11.8
Ti-NP 0.7%	71	102	8.8

In Fig. 7 the magnetization curves of the series of USPIONs derived from the 2-pyrrolidone-coated NPs are reported as a function of the applied magnetic field at 300 K and 5 K. Also in this case, the values of the magnetization of the Titanium-based nanoparticles are larger than the native nanoparticles, namely the Py-NPs, as reported in Table 2.

The trends of the Zero-field-cooled (ZFC) and field-cooled (FC) magnetic susceptibility curves of the Py-NPs and Ti-NPs, reported in Fig. 8, confirm that the presence of Titanium increase the superparamagnetic behavior of the nanoparticles.

4. CONCLUSIONS

Despite of different preparation, the two series of USPIONs present an increase of the magnetization and a more intense superparamagnetic behaviour when Titanium carbamate is on the nanoparticle surface replacing the oleate or 2-pyrrolidone coatings. This result is very interesting also for future MRI and biomedicine applications. A possible explanation of this trend is related to the role of the Titanium ions in increasing the crystalline order of the iron oxide nanostructure. Further investigations [31] are in progress in order to rationalize this behavior.

Table 2 – Saturation magnetization *Ms* (emu/g of Fe_2O_3) of NPs at 300 K and 5 K and blocking Temperature T_B(K) for the series derived from the Py-NPs.

Samples:	*Ms* (300K)	*Ms*(5K)	T_B
Py-NP	35	45	48.4
Ti-NP	83	107	42.4

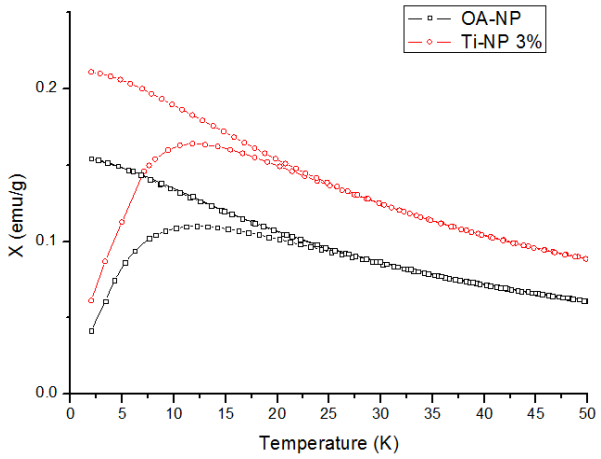

Fig. 5 – Zero-field-cooled (ZFC) and field-cooled (FC) magnetic susceptibility curves (emu/g of Fe_2O_3) of OA-NPs (squares) and $Ti(O_2CNEt_2)_4$-NP with [Ti] = 3 % (circles) measured at a magnetic field 100 Oe from 2 K to 50 K.

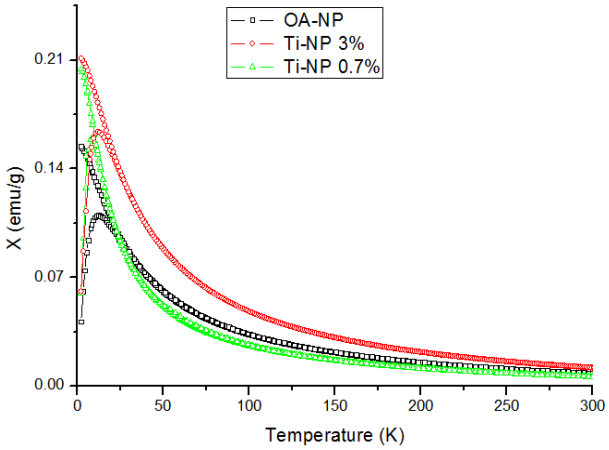

Fig. 6 – Zero-field-cooled (ZFC) and field-cooled (FC) magnetic susceptibility curves (emu/g of Fe_2O_3) of OA-NPs (squares), $Ti(O_2CNEt_2)_4$-NP with 3 % (w/w) of Ti (circles), $Ti(O_2CNEt_2)_4$-NP with 0.7 % (w/w) of Ti (triangles**)** measured at a magnetic field 100 Oe from 5 K to 300 K

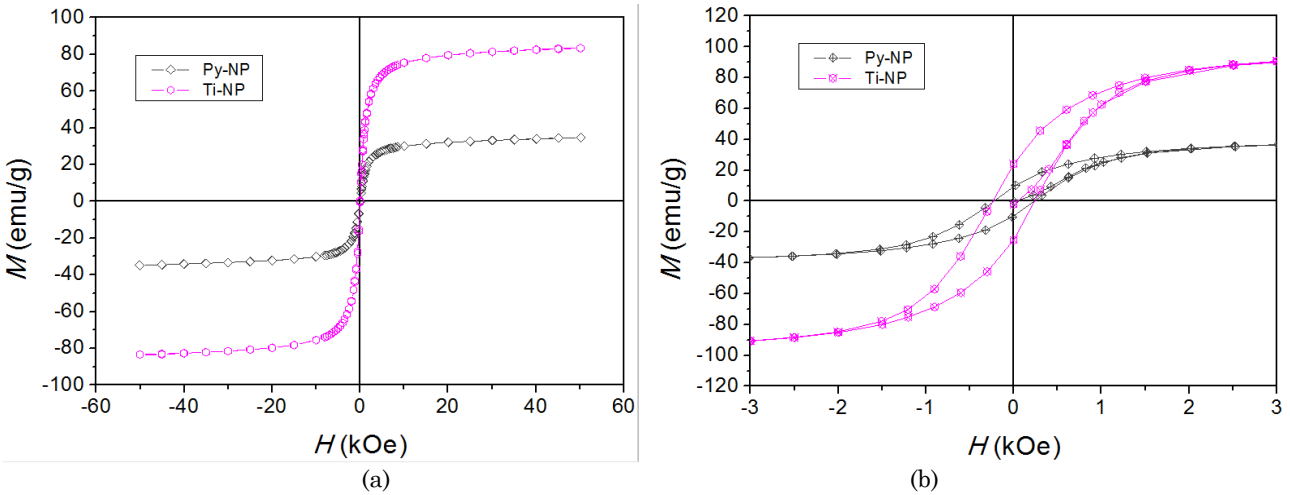

Fig. 7 – (a) Trend of the magnetization M (emu/g of Fe_3O_4) measured at 300 K as a function of the external magnetic field H (kOe) of the Py-NPs (black) and $Ti(O_2CNEt_2)_4$-NP (pink). (b) Trend of the magnetization M (emu/g of Fe_3O_4) measured at 5 K as a function of the external magnetic field H (kOe) of the Py-NPs (black) and $Ti(O_2CNEt_2)_4$-NP (pink).

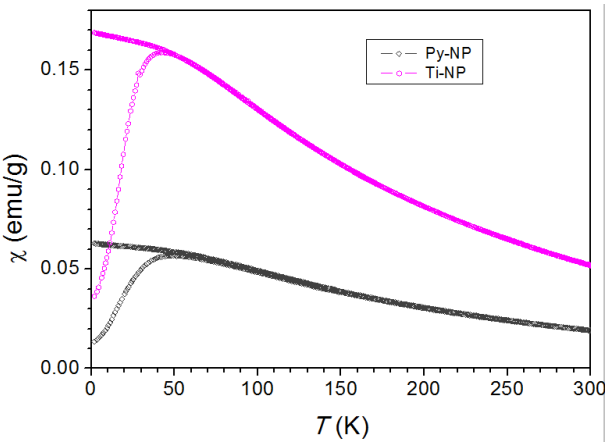

Fig. 8 – Zero-field-cooled (ZFC) and field-cooled (FC) magnetic susceptibility curves (emu/g of Fe_3O_4) of Py-NPs (black) and $Ti(O_2CNEt_2)_4$-NP (pink) measured at a magnetic field 100 Oe from 5 K to 300 K.

AKNOWLEDGEMENTS

S. Dolci thanks the IMAGO 7 Foundation for partial financial support and the "Galileo Galilei" Ph.D. School of the University of Pisa. V. Domenici thanks the L'Oreal Italia-Unesco grant "Women in Science 2010".

REFERENCES

1. J. Lodhia, G. Mandarano, N.J. Ferris, S.F. Cowell, *Biomed. Imaging Interv. J.* **6**, e12 (2010).
2. H. Fattahi, S. Laurent, F. Liu, N. Arsalani, L.V. Elst, R.N. Muller, *Future Nanomed.* **6**, 529 (2011).
3. N. Nitin, L. E. LaConte, O. Zurkiya, X. Hu, G. J. Bao, *J Biol. Inorg. Chem.* **9**, 706 (2004).
4. M. K. Yu, D. Kim, I.H. Lee, J.S. So, Y.Y. Jeong, S. Jon *Small* **7**, 2241 (2011).
5. Y. W. Jun, Y. M. Huh, J. S. Choi, J. H. Lee, H. T. Song, S. Kim, S. Yoon, K. S. Kim, J. S. Shin, J. S. Suh, J. Cheon *J. Am. Chem. Soc.* **127**, 5732 (2005).
6. E. Amstad, E. Reimhult *Nanomedicine* **7**, 145 (2012).
7. J. Xie, S. Jon, *Theranostics* **2**, 122 (2012).
8. M. Li, H. S. Kim, L. Tian, M. K. Yu, S. Jon, W. K. Moon, *Theranostics* **2**, 76 (2012).
9. P. Huang, Z. Li, J. Lin, D. Yang, G. Gao, C. Xu, L. Bao, C. L. Zhang, K. Wang, H. Song, H. Y. Hu, D. X. Cui *Biomaterials* **32**, 3447 (2011).
10. D. Peer, S. Hong, O. C. Farokhzad, R. Margalit, R. Langer *Nat Nanotechnol* **2**, 751 (2007).
11. J. Ruan, K. Wang, H. Song, X. Xu, J. Ji, D. Cui *Nanoscale Res. Lett.* **6**, 299 (2011).
12. R. Sun, J. Dittrich, M. Le-Huu, M. M. Mueller, J. Bedke, J. Kartenbeck, W. D. Lehmann, R. Krueger, M. Bock, R. Huss, C. Seliger, H. J. Gröne, B. Misselwitz, W. Semmler, F. Kiessling *Invest. Radiol.* **40**, 504 (2005).
13. H. Yim, S. Seo, K. Na *J. Nanomater*. Article ID 747196, (2011).
14. J. M. Perez, F. J. Simeone, A. Tsourkas, L. Josephson, R. Weissleder, *Nano Lett. 4*, 119 (2004).
15. J. M. Perez, T. O'Loughin, F. J. Simeone, R. Weissleder, L. Josephson *J. Am. Chem. Soc.* **124**, 2856 (2002).
16. S. Laurent, D. Forge, M. Port, A. Roch, C. Robic, L.V. Elst, *Chem. Rev.* **108**, 2064 (2008).
17. E. Fantechi, G. Campo, D. Carta, A. Corrias, C. D. Fernandez, D. Gatteschi, C. Innocenti, F. Pineider, F. Rugi, C. Sangregorio, *J. Phys. Chem. C* **116**, 8261 (2012).
18. C. Cannas, A. Musinu, A. Ardu, F. Orru, D. Peddis, M. Casu, R. Sanna, F. Angius, G. Diaz, C. Piccaluga, *Chem. Mater.* **22**, 3353 (2010).
19. S. Briceno, W. Braemer-Escamilla, P. Silva, G. E. Delgado, E. Plaza, J. Palacios, E. Canizales *J. Magn. Magn. Mater.* **324**, 2926 (2012).
20. Q. Song, Z. John, *J. Amer. Chem. Soc.* **134**, 10182 (2012).
21. Y. Ren, N. Li, J. Feng, T. Luan, Q. Wen, Z. Li, M.L. Zhang *J. Colloid Inter. Sci.* **367**, 415 (2012).
22. R. M. Wong, D. A. Gilbert, K. Liu, A.Y. Louie *ACS NANO* **6**, 3461 (2012).
23. R. M. Cornell, U. Schwertmann, In *The Iron-Oxides: Structure, Properties, Reaction, Occurrences and Uses*. (Wiley VCH Publisher, Second Edition. Weinheim: 2003).
24. H. Y. Liu, T. T. Wang, L. Y. Zhang, L. Li, Y. A. Wang, C.G. Wang, S. M. Su, *Chem.-A Eur. J.* **18**, 3745 (2012).
25. T. Hyeon, S. S. Lee, J. Park, Y. Chung, H. B. Na *J. Am. Chem. Soc* .**123**, 12798 (2001).
26. M. K. Yoo, I. Y. Kim, E. M. Kim, H.-J. Jeong, C.-M Lee, Y.Y. Jeong, T. Akaike, C. S. Cho, *J. Biomed. Biotechnol.* **2007**, 94740 (2007).
27. F. Calderazzo, S. Ianelli, G. Pampaloni, G. Pelizzi, M. Sperrle, *J. Chem. Soc. Dalton Trans.* 693 (1991).
28. E. B. Sandell, *Colorimetric determination of traces of metal*, 2nd ed., London: Interscience Publ.: 1950.
29. S. Dolci,V. Ierardi, A. Gradišek, Z. Jagličić, M. Remskar, T. Apih, M. Cifelli, G. Pampaloni, C. A. Veracini and V. Domenici, *Current Phys. Chem.* In press (2012).
30. V. Domenici, S. Dolci, V. Ierardi, Z. Jagličić, F. Pineider, A. Boni, M. Remskar, G. Pampaloni, C. A. Vera*cini, J. Mater. Sci.* submitted.
31. V. Domenici, S. Dolci, A. Boni, G. Pampaloni, et al. work in progress.
32. L. Calucci, C. Forte, G. Pampaloni, C. Pinzino, F. Renili, *Inorg. Chim. Acta* **363**, 33 (2010).
33. C. M. Sorensen. In: K. J. Klabunde, editor. *Nanoscale Materials in Chemistry*. New York: Wiley-Interscience, (2001) p. 205.